Design and Construction of Unmanned Aerial Vehicles Using Nano Aluminum and Carbon Composite Materials

Basel Ghurmullah Ahmed Almalki [1], Abdulaziz Mohammed Ammar Almutairi [1], Abdullah Awad Hamoud Alshammari [1], Faisal Adel Mohammed AlAbdulwahab [1]

[1] Department of Mechanical and Industrial Engineering, College of Engineering, Majmaah University, Al-Majmaah, Riyadh, 11952, Saudi Arabia

Abstract

This project aims to design and manufacture an unmanned aerial vehicle (UAV) structure using nano aluminum and carbon composite materials named "Arabian Leopard." Over the past period, the UAV market has experienced significant growth. In 2019, at least 60 countries were engaged in the development or implementation of at least 1,300 different drones. The Kingdom of Saudi Arabia is no exception; as a result, it prioritized this sector in Vision 2030 through investment and support to localize and develop it. The paper discusses the advantages of using these advanced materials, their impact on UAV design, and the challenges associated with their implementation. Various design considerations, manufacturing techniques, and structural analysis methods specific to the proposed materials are examined. The research presented in this paper lays the foundation for developing lightweight and robust UAVs that can revolutionize the unmanned aviation industry. The ANSYS fluent software will conduct a CFD simulation of the UAV design and airfoil. The airfoil CFD simulation is used to find the lift/drag characteristics of the airfoil used in the UAV design. In this CFD simulation, we conducted an airfoil simulation using Ansys Fluent software. From here, our project is to enhance the local content, present a unique design that embodies a national identity, and introduce nano-aluminum into the airframe to increase its durability, as the aerial vehicle (AV) is the primary component of the UAV system.

Keywords:

Unmanned Aerial Vehicle (UAV); Nano aluminum and carbon composite materials; Arabian Leopard; CFD simulation; National identity in design; ANSYS Fluent software.

Submitted: 6-APR-24

Accepted: 23-MAY-24

Published: 01- July-24

DOI: jeas.2024010505

Distributed under
Creative Commons CC-BY 4.0

OPEN ACCESS

1. Introduction

This study introduces Unmanned Aerial Vehicles (UAVs), carbon fiber, glass fiber, and Nano-aluminum. It discusses the types of UAVs, payload, and classification. Many titles are used to describe air vehicles, such as (UAV), radio-controlled (RC) planes, remotely piloted vehicles (RPV), model airplanes, drones, and remotely piloted aircraft (RPA). There is not much RPV usage currently, mainly because it is an older term. It is primarily hobbyists, aero-modelers, and the Academy of Model Aeronautics (the World's largest model aviation association) that use the terms "RC plane" and "model airplane" while the media uses the word "drone." In the past, drones were pilotless aircraft controlled by radio signals or aircraft that did not require a pilot to be on board [1]. The world has recently witnessed an increase in the popularity of UAVs or drones due to the diversity and versatility of their uses in military and civil fields such as exploration, search and rescue, oil platforms, medical uses, wireless communications, air surveillance, public security, military operations, agriculture, atmospheric sensing, infrastructure management, logistics, freight transportation, and wildfire monitoring [2, 3]. Air vehicles are complex systems that include structures, aerodynamic elements, propulsion systems, and control systems. Sensors and other payloads are also part of the complete system, communications packages, and launch and recovery subsystems. Air vehicles (AV) are essential to Unmanned Aerial Systems (UAS). It is important to recognize that the air vehicle is a part of the airborne Unmanned Aerial System, composed of the airframe, propulsion system, flight controls, and electric power system. In order to communicate data from the airborne portion of the communications data link, the air data terminal is mounted in the air vehicle. A payload is also carried by the air vehicle. However, it is generally regarded as an independent subsystem, which is interchangeable between different aircraft and is often designed to accomplish one or more missions an aircraft can perform. Fixed-wing aircraft, rotary-wing aircraft (single or multiple), and ducted fans are all examples of air vehicles. It is also possible for lighter-than-air vehicles to be referred to as UAVs. Therefore, our project needs to develop and improve the structure by adding nano-aluminum to the vehicle, which will be discussed later in the introduction. **Fig. 1** shows a key-shot rendered picture of a UAV, which would be a high-quality, realistic image showcasing the UAV's design, features, and materials. It provides a visually appealing representation, highlighting the aircraft's aesthetics and intended use.

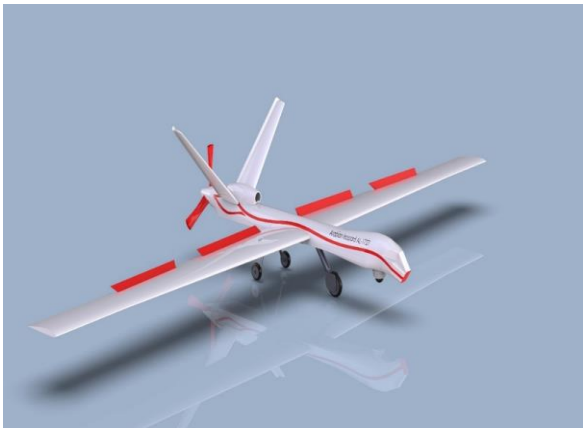

Fig. 1. The key shot rendered a picture of the UAV.

Classification of UAV

Fig. 2 shows UAVs can be classified based on size, endurance and range, engine type and power, altitude, number of rotors, cost, and payload. [4].

The use of advanced materials in UAV technology has the potential to greatly enhance the performance, efficiency, and durability of unmanned aerial vehicles. By incorporating nano aluminum and carbon composite materials, UAVs can benefit from their unique properties, such as high strength-to-weight ratio, excellent thermal stability, and corrosion resistance.

The lightweight nature of these materials enables UAVs to carry larger payloads, extend flight times, and increase maneuverability. Additionally, their enhanced structural integrity and aerodynamic efficiency improve stability, precision, and flight performance. These advancements have significant implications for various UAV applications, including surveillance, agriculture, disaster management, and delivery services.

However, adopting nano aluminum and carbon composite materials in UAV design also presents challenges. These include cost considerations, manufacturing complexities, regulatory compliance, and safety concerns. Addressing these challenges requires further research, technological advancements, and collaboration between academia, industry, and regulatory bodies. By exploring the design considerations, manufacturing techniques, structural analysis methods, and case studies related to the use of nano aluminum and carbon composite materials in UAV construction, this topic contributes to the

growing body of knowledge in this field. It sheds light on the potential benefits and challenges of implementing advanced materials, paving the way for future innovations and advancements in UAV technology.

Overall, the exploration of advanced materials in UAV technology represents an exciting and developing area that holds great promise for revolutionizing the capabilities and applications of unmanned aerial vehicles.

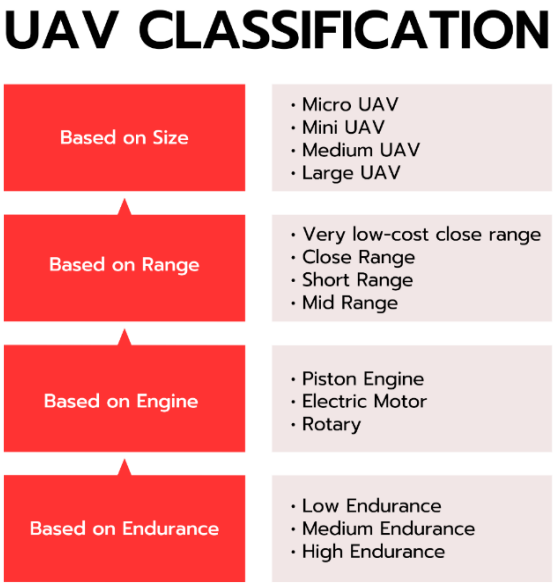

Fig. 2. UAV Classification is based on size, range, engine, and endurance [5].

Micro UAV Size is a manned aerial vehicle that is between 30-50 cm long, similar to a large insect. There is a growing trend towards micro-sized UAVs that resemble insects, with wings that flap or rotate. It can be used for spying or biological warfare since it is very small, light, and highly effective. In the case of larger aircraft, conventional aircraft configurations are applied, as shown in Table 1. Depending on the desired maneuverability, one should choose flapping or rotary wings. Perches and landing can be accomplished on small surfaces by using flaps [6]. A small UAV is an unmanned aerial vehicle with dimensions greater than 50 cm and less than 2 meters. They are also sometimes called mini-UAVs. Fixed-wing models are standard in this category, and most designs are thrown into the air by hand [6]. A medium-sized UAV is too heavy to be carried by one person but still smaller than a light aircraft. These aircraft have an average wingspan of about 5-10 meters and a payload capacity between 100 and 200 kilograms [7]. The table categorizes unmanned aerial vehicles (UAVs) based on their endurance and range capabilities, providing examples for each category. In the high category, UAVs have an endurance of over 24 hours and a range exceeding 1500 kilometers. Predator B is an example in this category, known for its long endurance and ability to conduct extended-range surveillance missions. In the medium category, UAVs have an endurance ranging from 5 to 24 hours and between 100 to 400 kilometers. The Silver Fox is an example of a medium-endurance UAV widely used for aerial mapping and surveillance applications. Lastly, in the low category, UAVs have an endurance of less than 5 hours and a range of less than 100 kilometers. The Pointer is an example in this category, typically utilized for short-range surveillance and monitoring tasks. Table 1 helps compare and understand the different categories of UAVs based on their endurance and range capabilities, with specific examples to illustrate each category.

Table 1. Classification based on range and endurance.

Category	Endurance	Range	Example
High	>24 hours	>1500 km	Predator B
Medium	5 - 24 hours	100 - 400 km	Silver Fox
Low	< 5 hours	< 100 km	Pointer

2. Problem Statement

During the final element, we encountered some problems in making the necessary build and tests for the model as the following:

- The utilization of nanoparticles, which are materials of a very small size.
- Safety is among the most important considerations when working with unmanned aerial vehicles (UAVs). To prevent landing collisions, UAVs must be programmed with "detect and avoid" capabilities equivalent to those of manned aircraft.
- Unmanned aerial vehicles cause problems with the overall budget because they are exceedingly expensive to develop and maintain (the costs may decrease over time).

- However, unmanned aerial vehicles (UAVs) have several issues, including limitations in terms of endurance and difficulty, transportation, construction, and design. The batteries used in UAVs are cumbersome and huge, and they drain very quickly. Meanwhile, engines that run on gasoline produce a lot of noise and emissions.

The current state-of-the-art materials used in UAV construction include aluminum alloys and carbon fiber composites. Aluminum alloys balance strength, weight, and cost, while carbon fiber composites offer high strength-to-weight ratios.

Nano aluminum and carbon composites offer potential advantages in UAV construction. Incorporating nano aluminum particles enhances the mechanical properties of composites, such as strength and toughness, without significantly increasing weight. This enables the construction of lightweight UAVs with improved durability. Combining carbon composites with nano aluminum provides synergistic effects, reducing weight, increased strength, enhanced maneuverability, and extended flight endurance. These advanced materials push the boundaries of UAV performance, enabling longer missions and greater payload capacity.

3. Experimental Details

This study focuses on 1k Carbon Fiber Cloth, Epoxy Laminating Resin, Twill Woven Glass Cloth, carbon fiber and glass fiber wet lay-up method, and UAV design.

Materials

For the aerodynamics and weight goals, lightweight carbon fiber, light glass fiber, appropriate epoxy material, and nano aluminum powder were selected. This section will provide details on these materials. To achieve the desired shape of the target component, manufacturing methods are designed to combine resin matrixes with reinforcement fiber mats to ensure no voids and maximum resin-fiber wetting.

Methods

The desired shape of the target component and manufacturing methods are designed in a way that allows resin matrixes to be combined with reinforcement fiber mats to ensure that there are no voids and there is maximum resin-fiber wetting. Due to this, many composite processing methods aim to achieve maximum wet-out to meet component performance requirements. Process parameters, such as applied pressures and cure temperatures, determine the degree of resin impregnation. Several factors affect the outcome of a part, including reinforcement permeability, fiber volume fraction, resin curing kinetics, viscosity, and part dimension and complexity. These factors should be revealed as a function of process parameters to produce high-quality parts [8].

Hand lay-up method

A combination of glass fiber, carbon fiber, and a liquid thermosetting resin is layered on the surface of a male or female mold using a hand lay-up process procedure. In the next step, the part is cured at room temperature or heated to accelerate the process. The thickness is built up by manually laying fiber-reinforced material and applying resin to the mold. Using hand or roller pressure, trapped air is removed. The mold should be clamped with a rubber bag. Mold and bag are vacuumed to remove trapped air between the resin and reinforcement.

EL2 Epoxy Laminating Resin

With its low viscosity, this epoxy resin is particularly effective for carbon and aramid fiber (Kevlar) reinforcement because it does not cause air bubbles to form in a laminate as easily as other epoxy systems [9].

Nano-Aluminum Powder

The white powder consists of nanoparticles of aluminum oxide in the alpha phase with a purity of 99.9%, APS Size 200 nm, SSA 8-10 m2/g, white Color, rhombohedral Structure, m.p. 2045oC, b.p. 2980oC, and density 3.97 g/cm3 [10].

Synthesis Of Epoxy

An amount of epoxy is placed approximately equal to the weight of the fabric, for example, 90g of carbon fiber. A 90 g mixture of epoxy, 30% Hardener, and 1% nano aluminum is placed on top. After 24 hours of vacuuming at room temperature, the part can be used with a layer thickness of approximately 2 mm [11].

UAV design

SolidWorks was used to design the UAV model and molds, and a key shot was used to make the color image of a UAV. A CNC machine made the molds from water-resistant green MDF wood [12-14]. This section will discuss the UAV structure and molds.

UAV Structure Model

A UAV (Unmanned Aerial Vehicle) structure model is a detailed representation of the physical framework and components that form the aircraft, as shown in **Fig. 3**. It encompasses the arrangement and organization of key structural elements, including the fuselage, wings, tail, control surfaces, landing gear, and payload bay [15-17]. The fuselage serves as the main body, housing essential systems and payload, while the wings generate lift and provide stability. The tail section comprises horizontal and vertical stabilizers, contributing to stability and control. Control surfaces, such as ailerons, elevators, and rudders, enable maneuverability. The landing gear facilitates safe takeoff, landing, and ground operations, while the payload bay accommodates mission-specific equipment [18-19]. The structure model is crucial for engineering analysis, design optimization, and manufacturing, ensuring the UAV's structural integrity, weight distribution, and overall performance.

Engineers consider various factors such as material selection, weight reduction, and aerodynamic considerations when developing a UAV structure model. Advanced modeling techniques, including computer-aided design (CAD) software, are utilized to visually represent the UAV's structure, as shown in **Figs. 4 & 5**. This allows for precise visualization, analysis, and simulation of the aircraft's behavior under different conditions.

The structure model serves as a blueprint for manufacturing processes, enabling the fabrication and assembly of the UAV's components. Through iterative design iterations and testing [20-24], engineers aim to optimize the structure model to meet performance objectives, such as durability, stability, and payload capacity, while ensuring compliance with safety regulations and operational requirements.

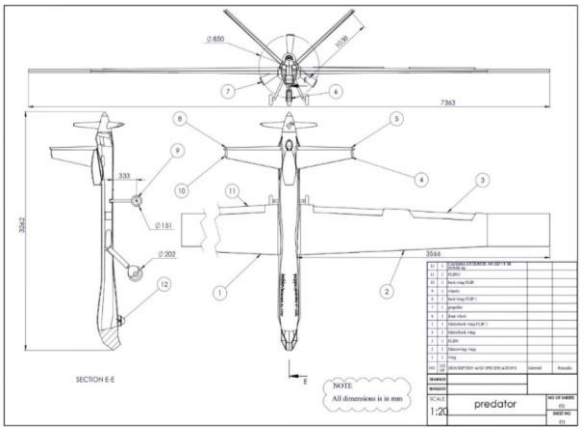

Fig. 3. The parts and dimensions of UAV structure.

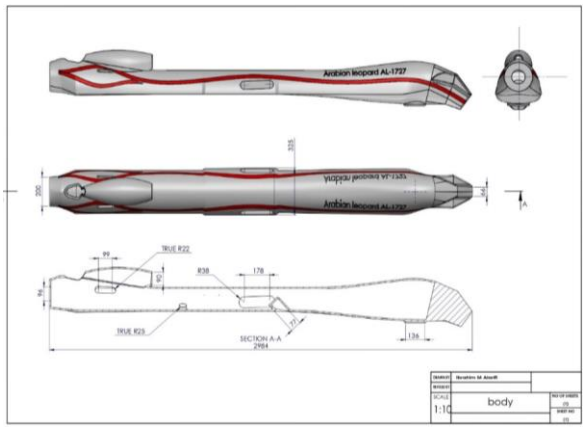

Fig. 4. Body and all view dimensions.

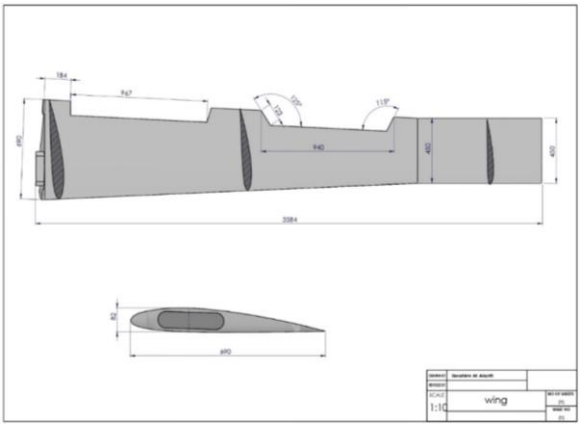

Fig. 5. The wing top and front view dimensions.

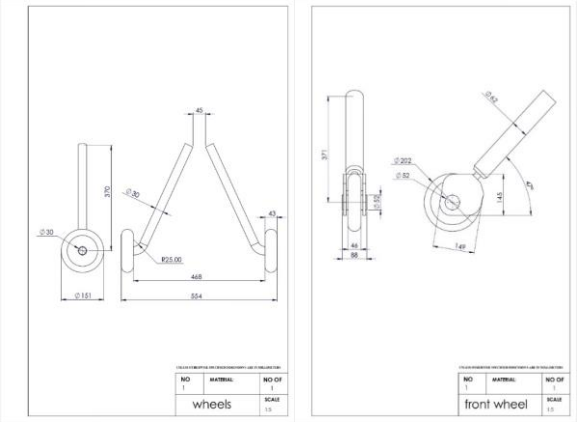

Fig. 6. The wing top and front view dimensions.

Fig. 6 shows the dimensions of wheels and landing gear for a UAV depending on factors such as the aircraft's weight, size, terrain, operating conditions, takeoff/landing requirements, payload, and transportation considerations [25-27]. Proper ground clearance, support, and stability are essential for safe operations. Specific design specifications and guidelines should be consulted to determine the appropriate dimensions for a particular UAV.

UAV Internal Structure

The internal structure, which consists of several parts such as ribs, spars, frames, and tubes, was made using SolidWorks to match the UEV design, as shown in **Fig. 7**. This section will show the parts of the internal structure.

Fig. 8 shows 18 ribs in the wing, each of different dimensions, with two slots for the main and rear spar. Each rib contains holes of various diameters to pass tubes and electrical wires, as shown in **Fig. 9**.

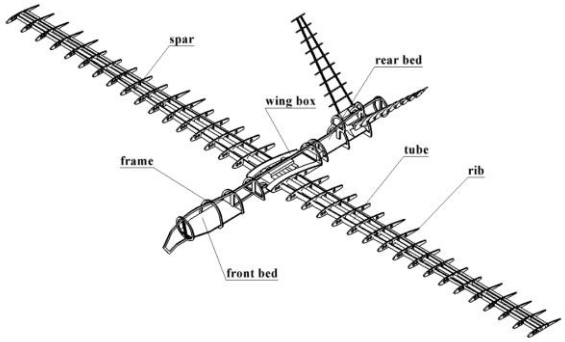

Fig. 7. The isometric view of the internal structure shows all parts.

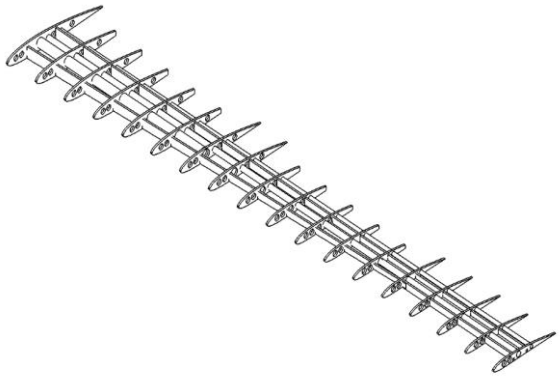

Fig. 8. The internal structure of the wing shows ribs and spars.

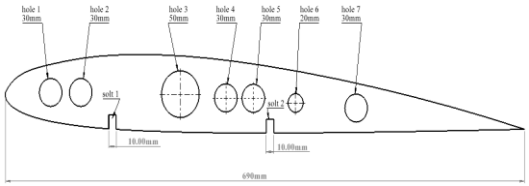

Fig. 9. The internal structure of the wing shows ribs and spars.

CFD Simulation of Airfoil and UAV Body Using ANSYS Fluent

Here are the steps in conducting the incompressible fluid flow CFD simulation of a UAV using ANSYS Fluent software. A CFD (Computational Fluid Dynamics) simulation is a computational technique used to analyze and predict the behavior of fluid flow, heat transfer, and other related phenomena. In the context of the given statement, a CFD simulation is being conducted on the airfoil and the body of the UAV (unmanned aerial vehicle) using Ansys Fluent software. The airfoil is a key component of an aircraft's wing, generating lift and controlling airflow around the wing.

By conducting a CFD simulation of the airfoil, engineers can analyze its aerodynamic performance, including lift and drag characteristics [28, 29]. This simulation helps understand how the airfoil design interacts with the surrounding air, allowing for optimization and improvements in efficiency and performance. Similarly, the CFD simulation is also

applied to the UAV body. The UAV body refers to the main structure or frame of the unmanned aerial vehicle.

By subjecting the UAV body to a CFD simulation, engineers can analyze the flow of air around the body, identify areas of turbulence, and optimize the design for improved aerodynamic performance. This simulation enables engineers to study the effects of different design modifications and materials on the UAV's overall efficiency, stability, and maneuverability. Ansys Fluent is a widely used software tool for conducting CFD simulations. It provides comprehensive features and capabilities to analyze and visualize fluid flow and heat transfer phenomena. By utilizing Ansys Fluent, engineers can accurately simulate and predict the behavior of airflows around the airfoil and UAV body, leading to informed design decisions and enhanced performance of the UAV.

Geometry of Airfoil

In this section, the CFD simulation of the whole UAV design and airfoil will be conducted using Ansys fluent software. Let's first discuss the airfoil CFD simulation to find the lift/drag characteristics of the airfoil used in the UAV design. In this CFD simulation, we conducted the simulation of airfoil using Ansys fluent software. The process started by first creating the simulation domain around the airfoil, which acts as the fluid domain for the simulation. In the image below, you can see the airfoil simulation with the domain. Then, heading forward, we can see the table showing the surface airfoil properties. We can also see the bounding box dimensions with the mesh statistics.

Mesh of Airfoil

Here, we can see the mash quality around the air flight we created in the fluid domain. The messages are structured here with the inflation layers applied to the airfoil's top and bottom surfaces to capture the flow properties around the airfoil. **Fig. 10** below shows the zoomed view of the mesh. We can see the inflation layers around the air and a structured mesh around the airfoil in the fluid domain.

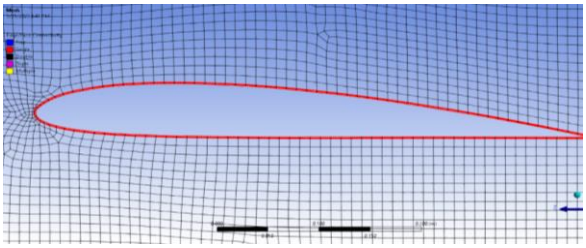

Fig. 10. Close-up view of the mesh of airfoil.

The following table shows the match properties we assembled for the airfoil. We can see the sizing quality and the mesh statistics here. We can see that we have assigned the linear element order and have a solver preference set as fluent, with the element size ranging from one exponent minus 2 meters.

Named Selection Fluid Domain of Airfoil

As we proceed with the setup, we must assign a boundary condition like this to the inlet-outlet. So, we selected the following images for the inlet-outlet walls, airfoil bottom surface, and walls. We have to assign these name selections and the simulation setup so that we can assign each of these pressure velocities or wall values. So, the first image shows us the inlet Nam selection, and the next shows the wall selection. **Fig. 11** shows the outlet of selection, the airfoil top surface selection, the airfoil bottom surface selection, and the last one shows us the fluid domain around the airfoil in red.

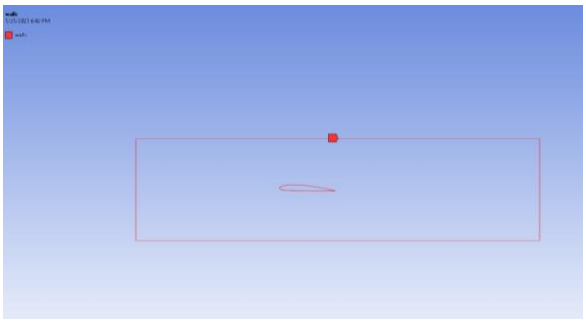

Fig. 11. The walls of the fluid domain.

After the named selection is applied to the fluid domain, we will select the solution method to use to solve the simulation; for the airfoil and UAV body, we have chosen the following attached solution methods in both simulations.

Solution of Airfoil

The viscous model for the simulation is Spalart Allmaras (1 equation), with the production model being velocity-based. The model was selected for its quick converging characteristics for airfoil-related simulations. We have chosen air as the fluid domain material and assigned it to the zone named domain, as seen in the image below. We selected an aircraft speed of around 86 m/s (310 Km/h) absolute for the velocity inlet. The aircraft speed is depicted as the velocity inlet at the inlet named selection. After the boundary conditions and simulation setup are completed, the simulation starts. Here, we can see the solution converging as the iteration increases. **Fig. 12** shows the simulation stops after a specific residual value, showing that the solution has converged sufficiently.

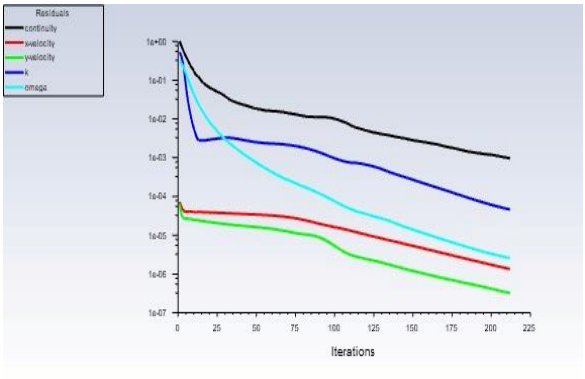

Fig. 12. The residuals monitoring.

Also, the Coefficient of Lift and Coefficient of Drag of airfoil values are generated from the simulation as a result of control applied during the simulation process, which can be seen in the following two images.

4. Results and Discussion

The maximum pressure is the stagnation pressure generated at the tip of the UAV and its cowling. However, the cowling is fully packed due to CFD complexities, creating this pressure, as shown in **Fig. 13**.

The velocity contours show the boundary layer generation at the skin of the UAV with the no-slip condition. The maximum velocity remains at 86.11m/s, as shown in **Fig. 14**.

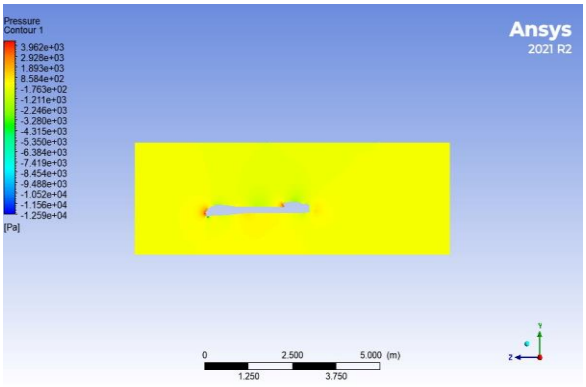

Fig. 13. The pressure contours of UAV.

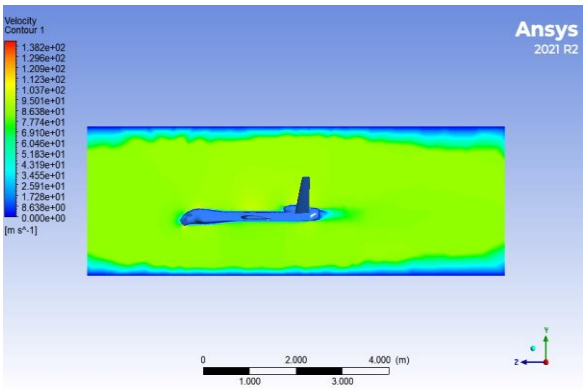

Fig. 14. The velocity contours of UAV.

Results of Airfoil CFD

Figs. 15 & 16 show the results of the airfoil CFD simulation provide valuable insights into the aerodynamic performance of the airfoil. Key outcomes include lift and drag coefficients, which quantify the lift generation and resistance to airflow, respectively. The pressure distribution across the airfoil surface reveals high and low-pressure areas, aiding in understanding the airflow behavior. The velocity distribution illustrates how the airflow varies along the airfoil, indicating regions of acceleration and deceleration. Detecting flow separation and stall phenomena helps optimize the airfoil design. Additionally, the boundary layer behavior analysis provides information on skin friction drag and heat transfer. These results empower engineers to make informed decisions regarding airfoil design modifications and enhance the overall efficiency and performance of the airfoil.

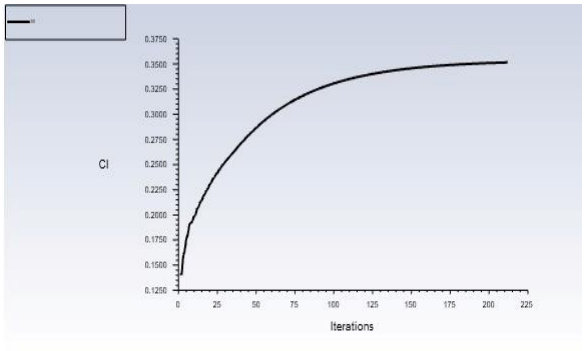

Fig. 15. The coefficient of lift of airfoil.

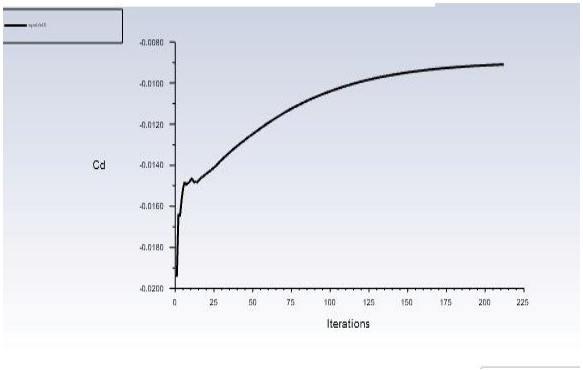

Fig. 16. The coefficient of drag of airfoil.

Also, the results, i.e., pressure contour and velocity contour around the airfoil and fluid domain, are shown in the following **Figs. 17 & 18**, showing the maximum air speed of 115 m/s at the top of the airfoil, showing the air acceleration and a lesser velocity than applied at the lower surface of the airfoil, showing the deceleration, which is the design consideration of cambered airfoils. Also, pressure decreases at the top airfoil surface and increases at the lower surface, creating the lift force, as shown in **Fig. 19**.

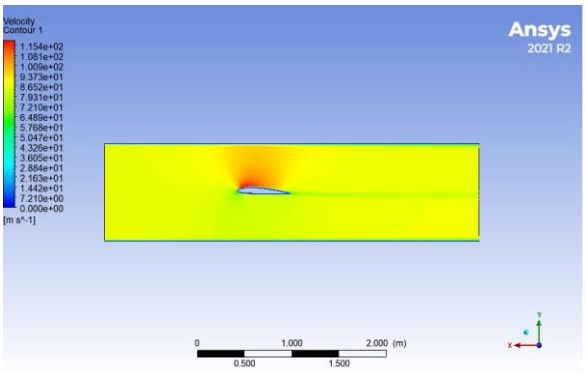

Fig. 17. The velocity contours.

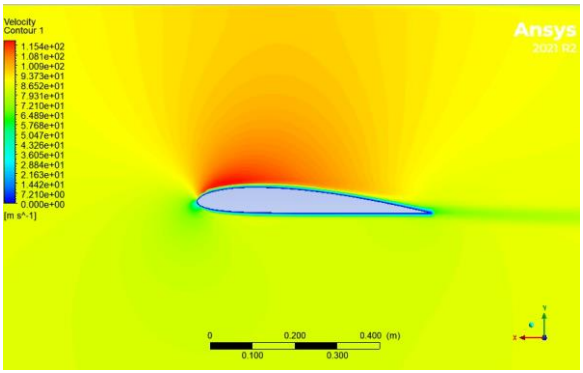

Fig. 18. The velocity contours close-up view.

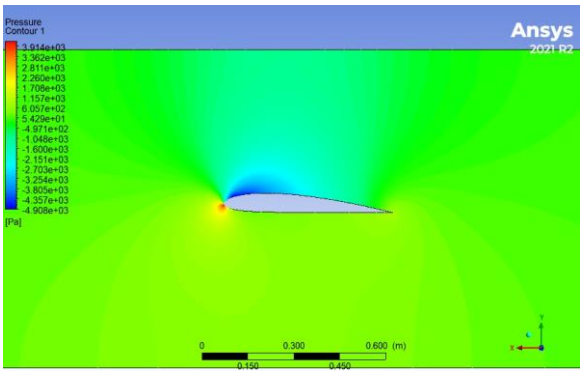

Fig. 19. The pressure contours.

Table 2 specifies the velocity as 86.11 m/s, given the boundary conditions. This value represents the magnitude of the airflow velocity applied to the CFD simulation of the airfoil or UAV body. It defines the speed at which the air flows around the object during the simulation. The response to these boundary conditions is provided in terms of two parameters: Cl and Cd. Cl (Coefficient of Lift) is a dimensionless parameter representing the lift generated by the airfoil or UAV body. In this case, the response indicates a Cl value of 0.35. The positive value of Cl suggests that the airfoil or UAV body is producing lift as the airflow passes over it. The magnitude of Cl provides information about the efficiency of the airfoil or UAV body in generating lift. Cd (Coefficient of Drag) is another dimensionless parameter representing the drag experienced by the airfoil or UAV body. The response mentions a Cd value of -0.009. The negative value of Cd implies that the airfoil or UAV body is experiencing a small amount of drag, which may indicate a relatively low resistance to the airflow. These parameters, Cl and Cd, play a crucial role in assessing the aerodynamic performance of the airfoil or UAV body. A higher Cl value indicates a more significant lift generation, which is desirable for

efficient flight. Conversely, a lower Cd value suggests a reduced drag, indicating improved aerodynamic efficiency. By analyzing these parameters, engineers can evaluate the design and make modifications to enhance the performance of the airfoil or UAV body in terms of lift and drag characteristics.

Table 2. Boundary Condition and response time for left force and drag force.

Boundary Condition	
Velocity	86.11 m/s
Response	
Cl	0.35
Cd	-0.009

Geometry of UAV

Similarly, we have applied the same steps we did for the airfoil simulation to the whole UAV body. The steps will remain almost the same, but with boundary conditions changed. The image below shows the fluid domain around the UAV body for conducting the CFD simulation. The UAV body is cut from the rectangular fluid domain to act as the UAV's outer surface. The remaining portion of the fluid domain acts as the air domain for the simulation, as shown in **Fig. 20**.

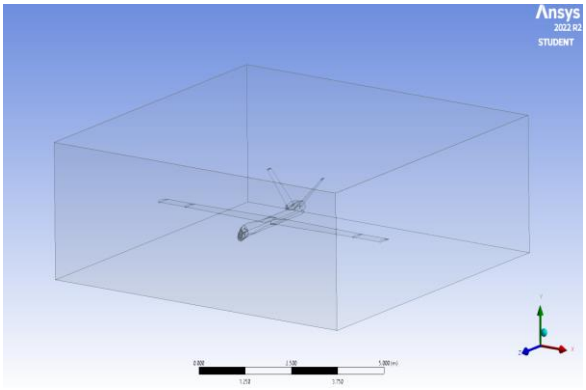

Fig. 20. UAV CFD Domain.

The mesh on the UAV and around the fluid domain is created with the following settings. The statement refers to making a mesh for the UAV (unmanned aerial vehicle) and the surrounding fluid domain in the CFD (Computational Fluid Dynamics) simulation. The mesh is a discretized representation of the computational domain, consisting of small geometric elements called cells or elements. The meshing process is a crucial step in CFD simulations as it divides the domain into finite elements to solve the governing equations for fluid flow. The settings used to create the mesh determine the quality and accuracy of the simulation results. While the specific settings are not mentioned, here are some common considerations when making a mesh.

Mesh Design

For mesh generation, the triangular method is chosen as it works all the time in complex geometries, while this method opts for the subject to keep the aspect ratio near 1 and skewness near zero, as shown in **Fig. 21**.

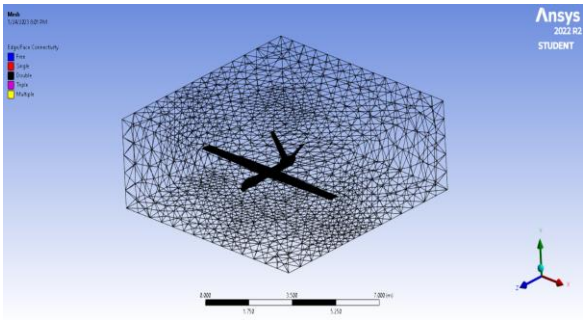

Fig. 21. The mesh of the UAV domain.

Named Selection

After that, the same method for assigning named selections is applied to the fluid domain. The named selections are inlet, outlet, walls, fluid domain, fuselage surface, wings surface, and tail surface, respectively, as shown in the following images in **Figs. 22 & 23**.

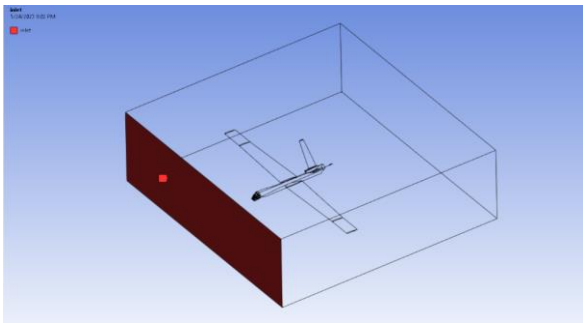

Fig. 22. The mesh of the UAV domain.

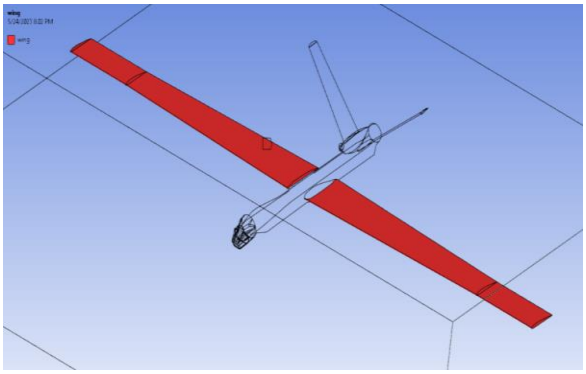

Fig. 23. The unnamed selection is Wing.

The steps after that are similar to those we took for the airfoil CFD simulation. **Fig. 24** shows the drag coefficient of a wing, a parameter that quantifies the amount of drag experienced by the wing as it moves through the air. It is a key factor in assessing the wing's aerodynamic efficiency, with lower values indicating reduced resistance to airflow. The drag coefficient is determined experimentally or through computational methods and plays a crucial role in aircraft design and performance optimization.

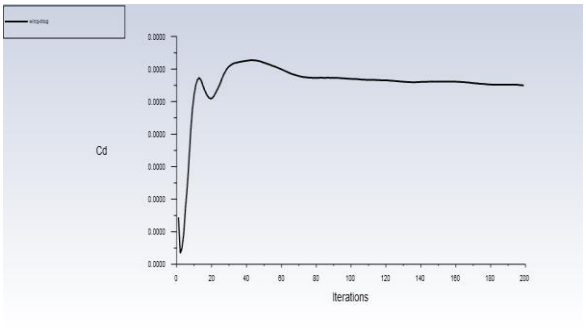

Fig. 24. The drag coefficient of the wing.

Fig. 25 shows the lift coefficient of a wing, which represents the amount of lift generated by the wing. It is a dimensionless value influenced by wing shape, angle of attack, and airfoil profile. The lift coefficient is determined through experimental measurements or computational methods and plays a vital role in evaluating the wing's aerodynamic performance and optimizing design.

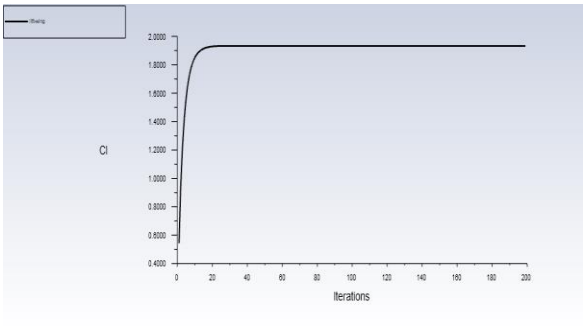

Fig. 25. The lift coefficient of the wing.

By monitoring the residuals, engineers can evaluate the solution's convergence and determine if further iterations are needed to achieve an accurate and stable solution. A well-converged solution is characterized by low and stable residuals, indicating that the equations are adequately solved and the solution is reliable.

Typically, residual monitoring involves tracking the residuals throughout the simulation and comparing them against predefined convergence criteria. These criteria can be based on specified tolerances or desired levels of accuracy. If the residuals fall below the convergence criteria, the solution is considered converged, and the simulation can be concluded. Otherwise, additional iterations or adjustments in the simulation settings may be necessary to achieve convergence. **Fig. 26** shows that residual monitoring is an essential part of UAV CFD simulations as it ensures the reliability and accuracy of the results. It helps validate the numerical solution and provides insights into its stability and convergence behavior. By carefully monitoring the residuals, engineers can gain confidence in the CFD results and make informed decisions regarding the design and performance of the UAV.

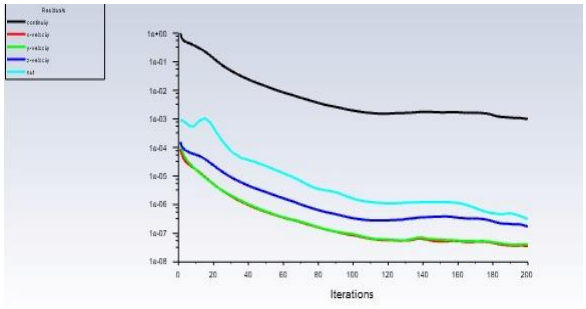

Fig. 26. Residual monitoring of UAV CFD.

Fig. 26 shows the residual monitoring in UAV CFD (Computational Fluid Dynamics), which refers to tracking and analyzing the residuals during the simulation. Residuals are the errors or imbalances in the governing equations (e.g., Navier-Stokes equations) that are solved numerically in the CFD simulation.

During the iterative solution process, the residuals are continuously monitored to assess the convergence of the solution. The residuals represent the difference between the computed values and the expected values of the variables (such as velocities, pressures, and turbulence parameters) at each computational cell or element.

5. Conclusions

In conclusion, as unmanned aircraft face new challenges due to technological advancements, it becomes crucial to thoroughly study and analyze them from all aspects. The CFD simulations focused on the airfoil and UAV skin and showed no adverse effects. The lift coefficient (Cl) was observed to be 0.12, indicating a relatively high lift generation, while the drag coefficient (CD) was found to be -0.0011, indicating low drag. The favorable ratio of a higher lift-to-drag coefficient suggests improved aerodynamic efficiency. Implementing the split-almirahs equation, a widely used approach in aerospace applications, has yielded highly accurate results. The solution obtained through the CFD simulations, including x-velocity, y-velocity, and continuity, has converted to a satisfactory level of 1x10-3, indicating stability and reliability in the analysis. However, it's important to note that the investigation focused on individual geometries, such as the wing, tail, and fuselage, analyzing their respective contributions to lift and drag.

Understanding the specific aerodynamic characteristics of each component is essential for optimizing the overall performance of an unmanned aircraft. By conducting detailed CFD simulations and analyzing the variables associated with separate geometries, researchers and engineers can gain valuable insights into the aerodynamic behavior of the UAV. This knowledge can guide the design and development process, allowing for improvements in lift, drag, stability, and overall efficiency. Ultimately, such comprehensive studies contribute to the advancement and successful implementation of unmanned aircraft technologies.

Data Availability

The data used to support the findings of this study are included in the article. Further data or information is available from the corresponding author upon request.

Declaration of Conflict Interest

The authors state that they have no recognized competing financial interests or personal relationships that could appear to have influenced the work described in this paper.

References

[1]. Otto, A., Agatz, N., Campbell, J., Golden, B. and Pesch, E., 2018. Optimization approaches for civil applications of unmanned aerial vehicles (UAVs) or aerial drones: A survey. Networks, 72(4), pp.411-458.

[2]. Cao, H.R., Yang, Z., Yue, X.J. and Liu, Y.X., 2017. An optimization method to improve the performance of unmanned aerial vehicle wireless sensor networks. International Journal of Distributed Sensor Networks, 13(4), p.1550147717705614.

[3]. de Lucena, A.N., da Silva, B.M.F. and Gonçalves, L.M.G., 2022. A micro aerial vehicle with basic risk of operation. Scientific Reports, 12(1), p.12772.

[4]. Arjomandi, M., Agostino, S., Mammone, M., Nelson, M. and Zhou, T., 2006. Classification of unmanned aerial vehicles. Report for Mechanical Engineering class, University of Adelaide, Australia, pp.1-48.

[5]. Çoban, S. and Oktay, T., 2018. Unmanned aerial vehicles (UAVs) according to engine type. Journal of aviation, 2(2), pp.177-184.

[6]. Harvey, M.C., Rowland, J.V. and Luketina, K.M., 2016. A drone with a thermal infrared camera provides high-resolution georeferenced imagery of the Waikite geothermal area in New Zealand. Journal of Volcanology and Geothermal Research, 325, pp.61-69.

[7]. Shichao, G., Dandan, G., Qiongyu, Z., Nankai, W. and Jiaxin, D., 2020, March. Research progress of anti-jamming technology of unmanned aerial vehicle (UAV) data link. In IOP Conference Series: Materials Science and Engineering (Vol. 816, No. 1, p. 012011). IOP Publishing.

[8]. Dharmendra, P., Chaithanya, K.J., Sameera, A., Kavathiya, K. and Monika, K.M., 2020. Design and analysis of an aircraft wing rib for different configurations. International Research Journal of Engineering and Technology, 7(6).

[9]. Jayaram, S., Boyer, L., George, J., Ravindra, K. and Mitchell, K., 2010. Project-based introduction to aerospace engineering course: A model rocket. Acta Astronautica, 66(9-10), pp.1525-1533.

[10]. Callister, W.D., Rethwisch, D.G., Blicblau, A., Bruggeman, K., Cortie, M., Long, J., Hart, J., Marceau, R. and Mitchell, R., 2007. Materials science and engineering: an introduction (Vol. 7, pp. 665-715). New York: John wiley & sons.

[11]. Johnson, D.J., 1987. Structure-property relationships in carbon fibres. Journal of Physics D: Applied Physics, 20(3), p.286.

[12]. Anoop, C.R., Singh, R.K., Kumar, R.R., Jayalakshmi, M., Antony Prabhu, T., Thomas Tharian, K. and Narayana Murty, S.V.S., 2021. A review on steels for cryogenic applications. Materials Performance and Characterization, 10(2), pp.16-88.

[13]. Corazza, P.H., Di Domênico, M.B., Facenda, J.C., Merlo, E.G., Borba, M. and Ozcan, M., 2022. Fiberglass versus cast metal posts: a practical review based on mechanical properties. Brazilian Dental Science, 25(4).

[14]. Plotino, G., Grande, N.M., Bedini, R., Pameijer, C.H. and Somma, F., 2007. Flexural properties of endodontic posts and human root dentin. Dental materials, 23(9), pp.1129-1135.

[15]. Kinney, J.H., Marshall, S.J. and Marshall, G.W., 2003. The mechanical properties of human dentin: a critical review and re-evaluation of the dental literature. Critical Reviews in Oral Biology & Medicine, 14(1), pp.13-29.

[16]. Cullen, J.K., Wealleans, J.A., Kirkpatrick, T.C. and Yaccino, J.M., 2015. The effect of 8.25% sodium hypochlorite on dental pulp dissolution and dentin flexural strength and modulus. Journal of Endodontics, 41(6), pp.920-924.

[17]. Sultan, Z., Sheikh, Z., Zafar, M.S. and Sauro, S., 2018. Dental Materials (Principles and Applications).

[18]. Teshigawara, D., Ino, T., Otsuka, H., Isogai, T. and Fujisawa, M., 2019. Influence of elastic modulus mismatch between dentin and post-and-core on sequential bonding failure. journal of prosthodontic research, 63(2), pp.227-231.

[19]. Calamia, J.R. and Calamia, C.S., 2007. Porcelain laminate veneers: reasons for 25 years of success. Dental clinics of north America, 51(2), pp.399-417.

[20]. Williams, K.R., Edmundson, J.T. and Rees, J.S., 1987. Finite element stress analysis of restored teeth. Dental Materials, 3(4), pp.200-206.

[21]. Lanza, A., Aversa, R., Rengo, S., Apicella, D. and Apicella, A., 2005. 3D FEA of cemented steel, glass and carbon posts in a maxillary incisor. Dental materials, 21(8), pp.709-715.

[22]. Novais, V.R., Quagliatto, P.S., Della Bona, A., Correr-Sobrinho, L. and Soares, C.J., 2009. Flexural modulus, flexural strength, and stiffness of fiber-reinforced posts. Indian journal of dental research, 20(3), pp.277-281.

[23]. Memon, S., Mehta, S., Malik, S., Nirmal, N., Sharma, D. and Arora, H., 2016. Three-dimensional finite element analysis of the stress distribution in the endodontically treated maxillary central incisor by glass fiber post and dentin post. The Journal of Indian Prosthodontic Society, 16(1), pp.70-74.

[24]. Elnaghy, A.M. and Elsaka, S.E., 2016. Effect of surface treatments on the flexural properties and adhesion of glass fiber-reinforced composite post to self-adhesive luting agent and radicular dentin. Odontology, 104, pp.60-67.

[25]. Murthy, I.N., Rao, D.V. and Rao, J.B., 2012. Microstructure and mechanical properties of aluminum–fly ash nano composites made by ultrasonic method. Materials & Design, 35, pp.55-65.

[26]. Braun, T., Schubert, A. and Zsindely, S., 1997. Nanoscience and nanotechnology on the balance. Scientometrics, 38, pp.321-325.

[27]. Müssig, J. and Haag, K., 2015. The use of flax fibres as reinforcements in composites. In Biofiber reinforcements in composite materials (pp. 35-85). Woodhead Publishing.

[28]. Li, Y., Xue, T., Li, R., Huang, X. and Zeng, L., 2018. Influence of a fiberglass layer on the lightning strike damage response of CFRP laminates in the dry and hygrothermal environments. Composite Structures, 187, pp.179-189.

[29]. Dobrzański, L.A., 2021. Advanced Composites with Aluminum Alloys Matrix and Their Fabrication Processes. Advanced Aluminium Composites and Alloys, p.3.